

Supplementary Materials for

Chimeric antibody targeting unique epitope on onco-Mucin 16 reduces tumor burden in pancreatic and lung malignancies

Supplementary Table 1: List of primers used in the study

Primer	Sequence
5E6-VH-F1	AATAGGGAATTGGAGGTGAAG
5E6-VH-R1	CCTTGGTGCTAGCTGAGGA
5E6-VL-F1	CCTTGGTGCTAGCTGAGGA
5E6-VL-R1	AGCCACCGTACGCTTTAT
VH seq	ATTAAGAGGAGAAATTAACC A
VL seq	AGGCCTCTAGATTAATGATGAT
pFUSE-CHIg/CLIg seq	TGCTTGCTCAACTCTACGTC

Supplementary Table 2: List of antibodies used in the study

ANTIBODIES	SOURCE	IDENTIFIER/DILUTION
List of primary antibodies used in Immunofluorescence		
E-cadherin	Santa Cruz	Cat# Sc-55510 (Ms) (1:100)
N-cadherin	Cell Signaling Technology	Cat# 13116S (Rb) (1:200)
M11	Agilent Dako	Cat# GA701 (Ms) (1:1000)
Actin Cytoskeleton / Focal Adhesion Staining Kit	Sigma	FAK100 (1:100)
pFAK (Y397)	Life Technologies	Cat # 700255 (Rb) (1:250)
List of secondary antibodies used in Immunofluorescence		
Alexa Fluor 568 goat anti-mouse IgG	Life Technologies	Cat#A11031 (1:300)
Alexa Fluor 568 goat anti-rabbit IgG	Life Technologies	Cat# A11011 (1:300)
Alexa Fluor 488 goat anti-mouse IgG	Life Technologies	Cat# A28175 (1:300)
Alexa Fluor 488 goat anti-rabbit IgG	Life Technologies	Cat# A11008 (1:300)
Alexa Fluor 488 goat anti-human IgG	Life Technologies	Cat# A-11013 (1:300)
List of antibodies used in Western Blotting		
N-cadherin	Cell Signaling Technology	Cat# 13116S (Rb) (1:1000)
E-cadherin	Cell Signaling Technology	Cat# 3195 (Rb) (1:1000)
Vimentin	Cell Signaling Technology	Cat#5741S (Rb) (1:100)

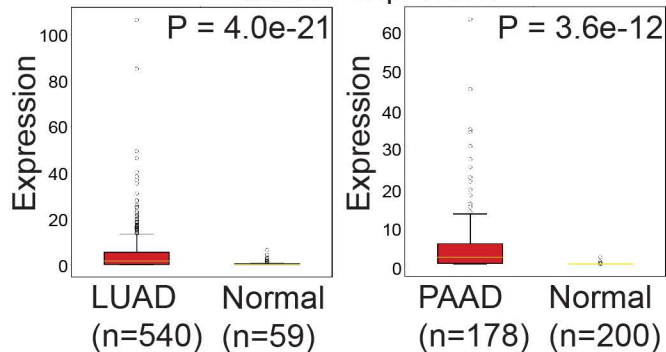
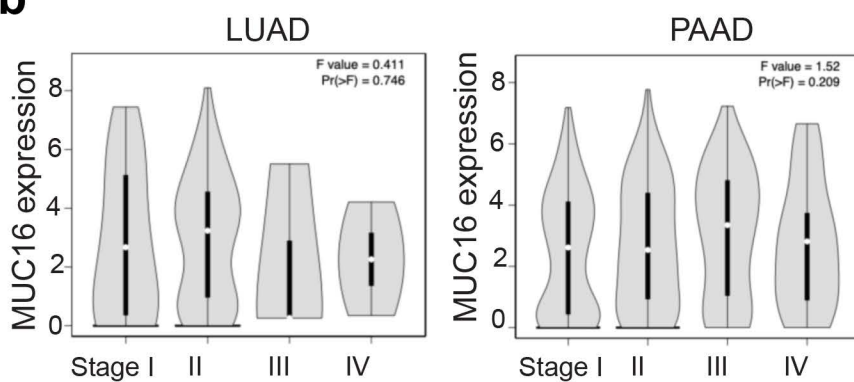
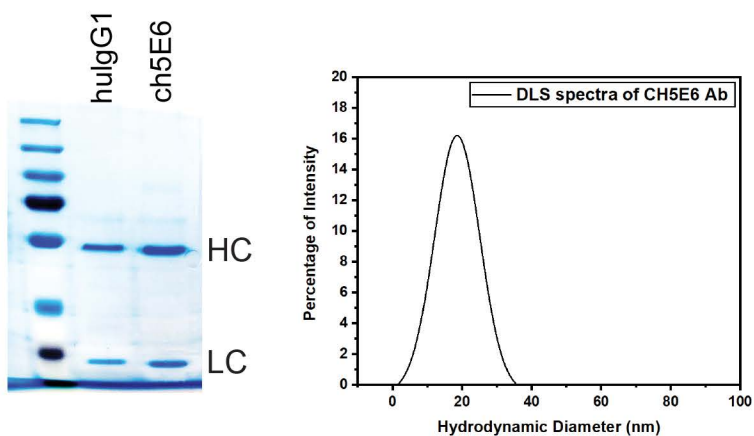
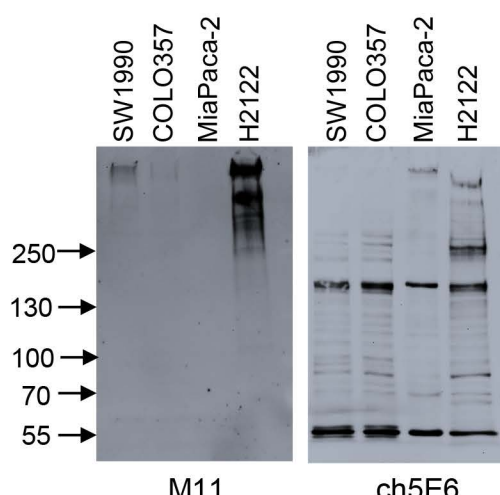
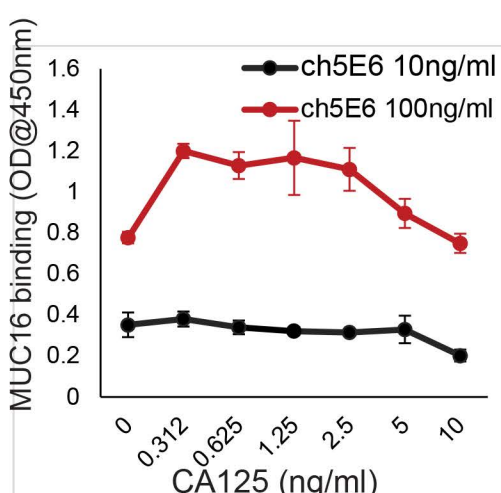
Fibronectin	ABclonal	Cat# A7488 (Rb) (1:1000)
p-P70S6K (T389)	Cell Signaling Technology	Cat# 9205 (Rb) (1:1000)
p-JNK	Cell Signaling Technology	Cat# 9251S (Rb) (1:1000)
pFAK (Y397)	Cell Signaling Technology	Cat#D20B1 (Rb) (1:1000)
P-p44/42 MAPK (Y202/204)	Cell Signaling Technology	Cat#9101S (Rb) (1:1000)
pAkt	Cell Signaling Technology	Cat#D9E (Rb) (1:1000)
Cyclin D	Cell Signaling Technology	Cat#92G2 (Rb) (1:500)

List of antibodies used in Immunohistochemistry

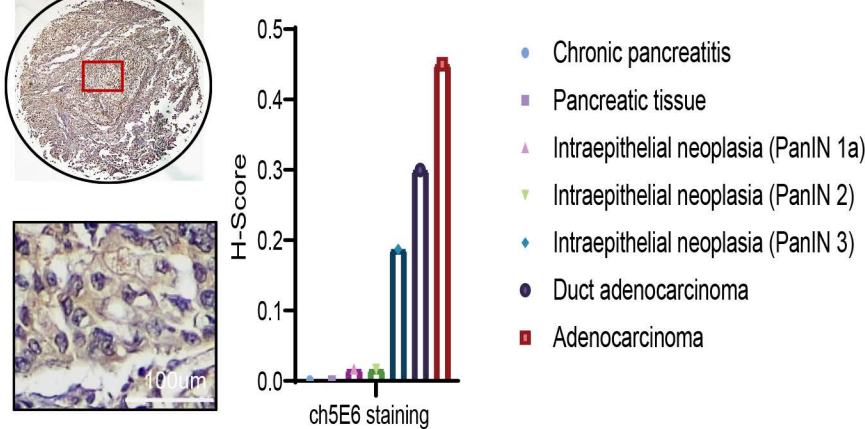
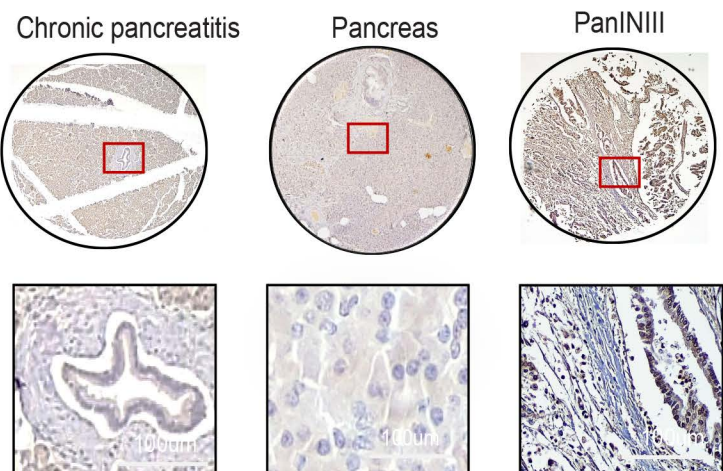
N-cadherin	Santa Cruz	Cat# Sc-55510 (Ms) (1:100)
M11	Agilent Dako	Cat# GA701 (Ms) (1:100)
Ki67	Cell Signaling Technology	Cat# D385 (Rb) (1:500)
Cleaved caspase 3	Cell Signaling Technology	Cat# D175 (Rb) (1:200)

a

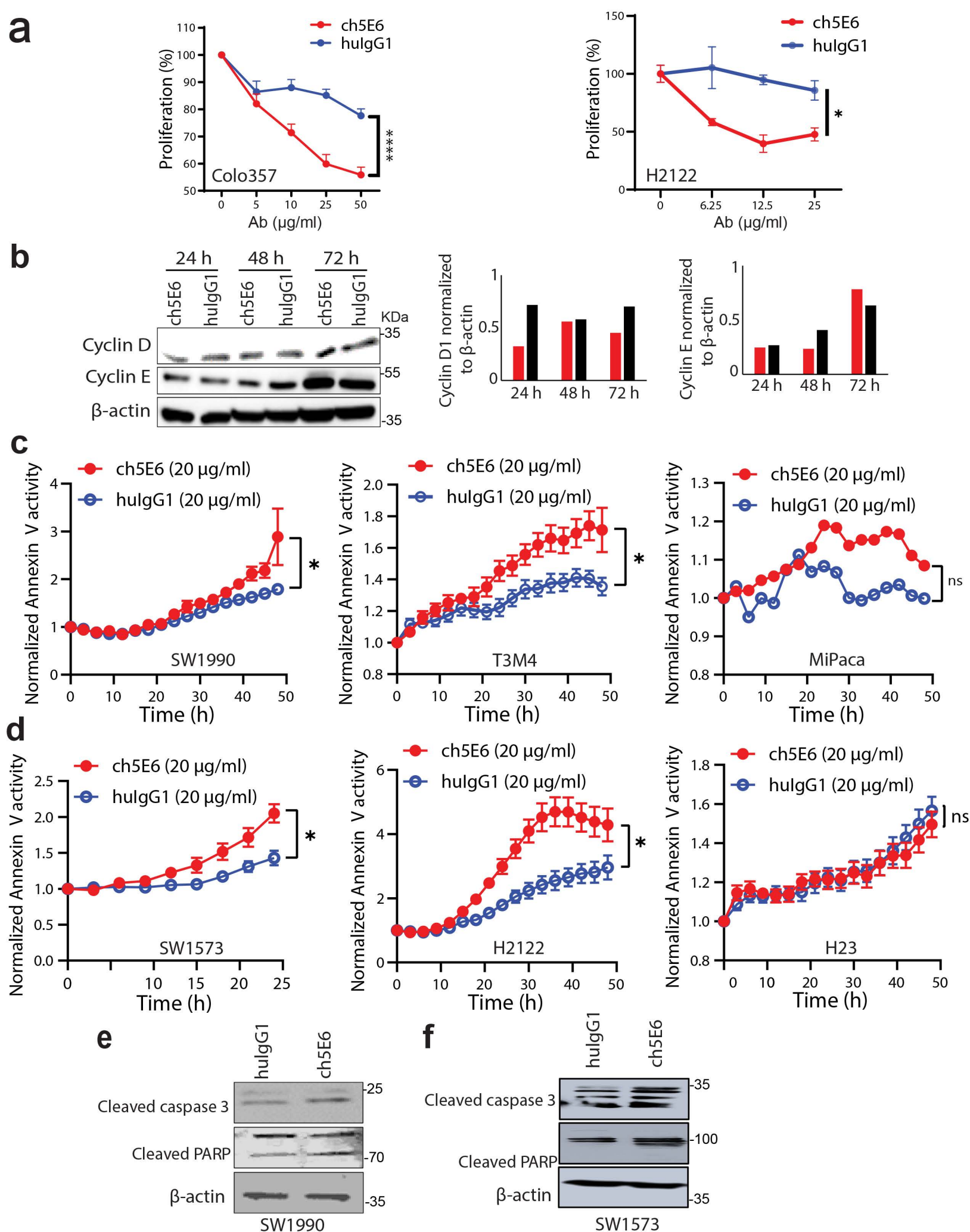
MUC16 expression

**b****c****d****e****f**

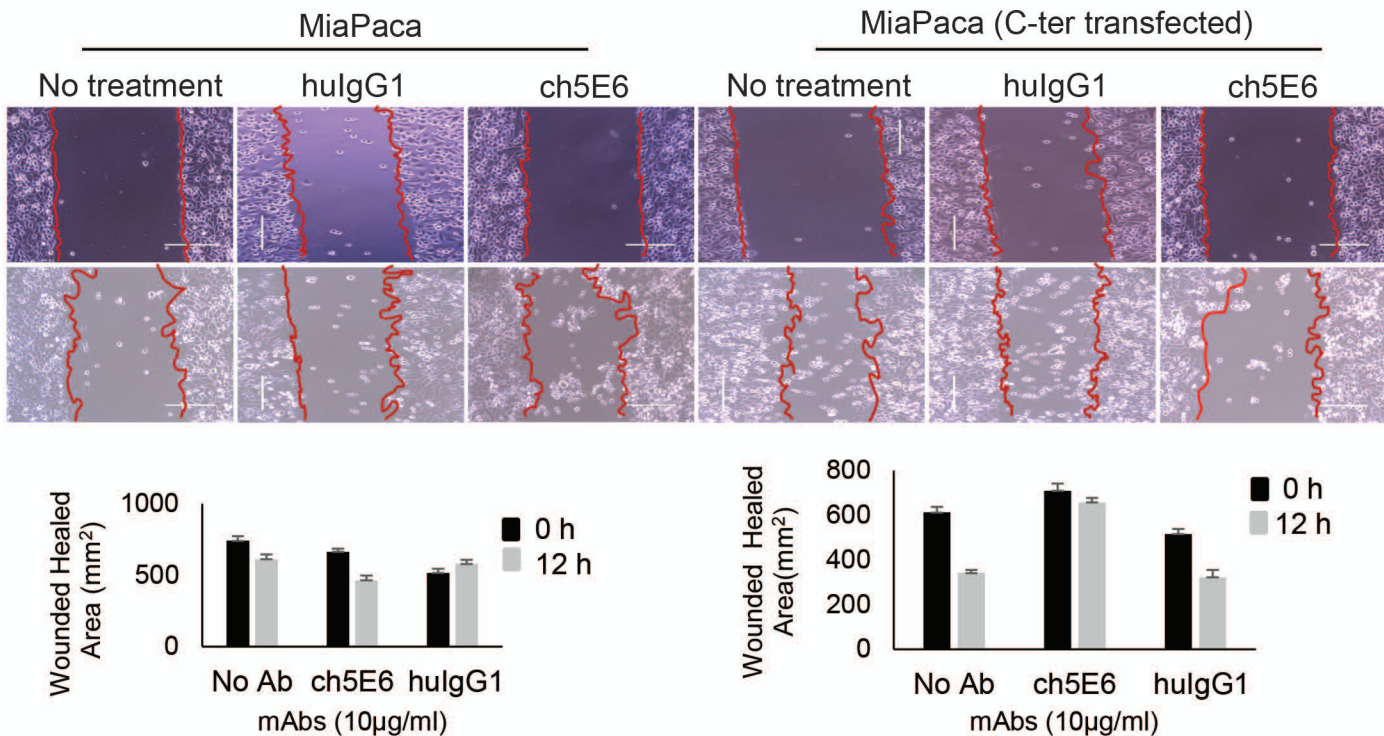
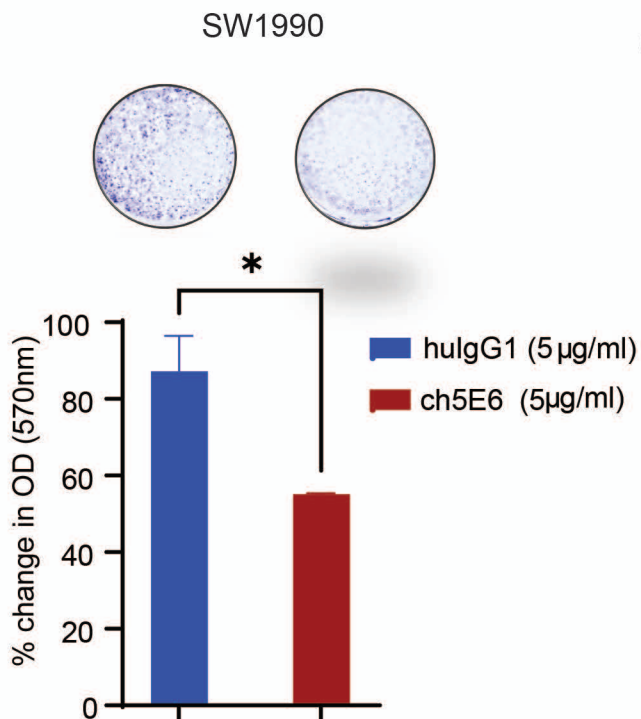
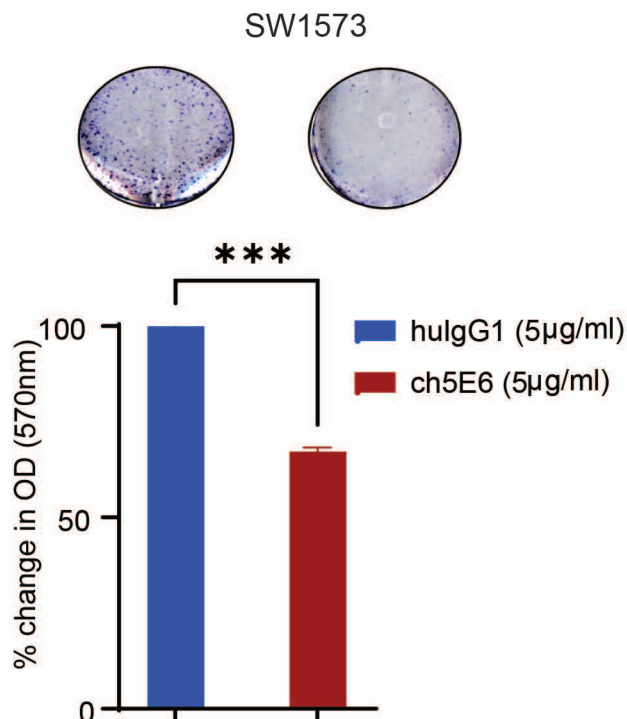
Cases	Number of cases	-	+	++	+++
NP	10	10	0	0	0
PDACs	69	14	18	28	9
NL	48	48	0	0	0
LUAD	48	13	16	8	5

g

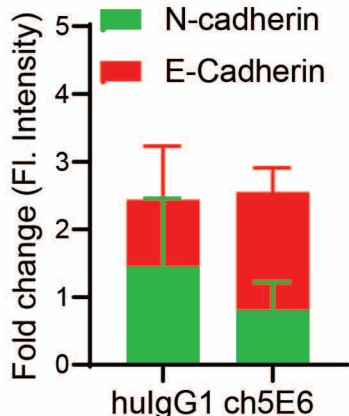
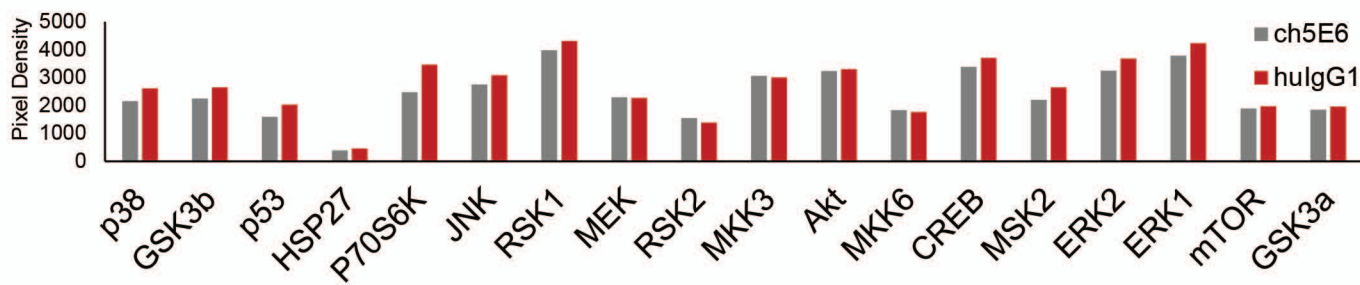
Supplementary Figure 1: **A.** Transcriptomic expression analysis of MUC16 in PDAC (Pancreatic Ductal Adenocarcinoma) patients (n=178) and adjacent normal (n=200) cases and NSCLC patients (n=540) along with adjacent normal cases (n=59) from GTEx datasets (<http://GEPIA.cancer-pku.cn>). **B.** Stage-specific expression of MUC16 in both PC and NSCLC patients showing its association with disease aggressiveness. **C.** The characterization of purified ch5E6 on Coomassie-stained gel showing the heavy and light chain bands of chimeric mAb5E6 at 50 and 25 kDa, respectively and Dynamic light scattering (DLS) showing a single peak at hydrodynamic diameter 16nm. **D.** Western blot analysis of cell lysates prepared after the collection of conditioned media showing a specific binding pattern of MUC16 with mAbM11 and ch5E6. Specific bands are indicated by arrow. **E.** Effect on MUC16 binding by ch5E6 in the presence of increasing concentrations of soluble CA125 from 0.3ng/ml to 5ng/ml. **F.** Table showing the percentage of tumors stained by ch5E6 in PC and NSCLC patients. **G.** Immunohistochemical staining of ch5E6 in chronic pancreatitis, PanIN1, PanIN2, PanIN3, and PDAC patients showing specific binding to MUC16 in PDAC patients. Scale bars, 100 μ m; *, P < 0.05; **, P < 0.005, ****, P < 0.0005.



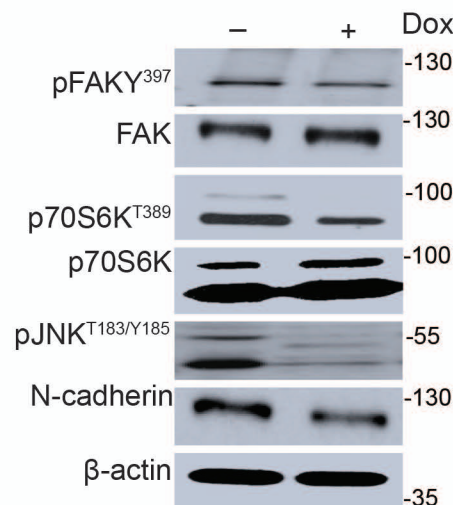
Supplementary Figure 2: **A.** Real-time MT glo assay showing a specific decrease in cell proliferation by ch5E6 treatment in COLO357 and H2122 cell lines. **B.** Immunoblot analysis of ch5E6 treated lysates for changes in the proliferation markers cyclins D and E at different time points from 24 hours to 72 hours. **C and D.** ch5E6 induced apoptosis in MUC16 expressing PC (SW1990, T3M4) and NSCLC cancer cell lines (SW1573 and H2122) as compared to isotype control mAb hulgG1. MUC16 negative lines MiaPaca-2-2 and H23 were not impacted by treatment. The representative images are shown in the lower panel for each cell line. **E and F.** The apoptosis was validated by increased levels of cleaved caspase 3 in chimeric mAb5E6 treated SW1990 and SW1573 cells. β -actin was used as loading control. Error bars indicate SEM. *, P < 0.05; **, P < 0.005

a**b****c**

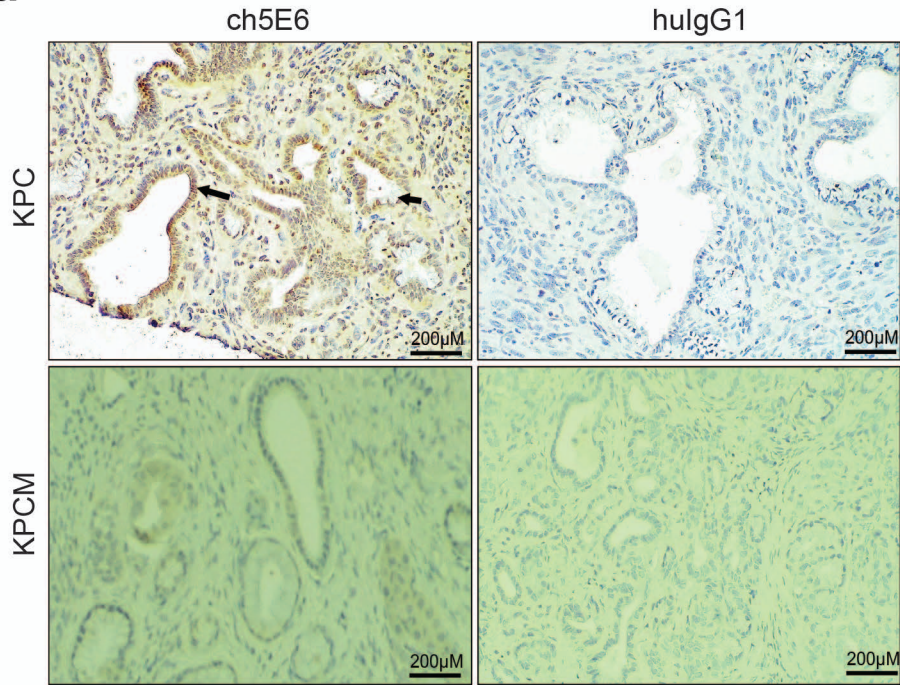
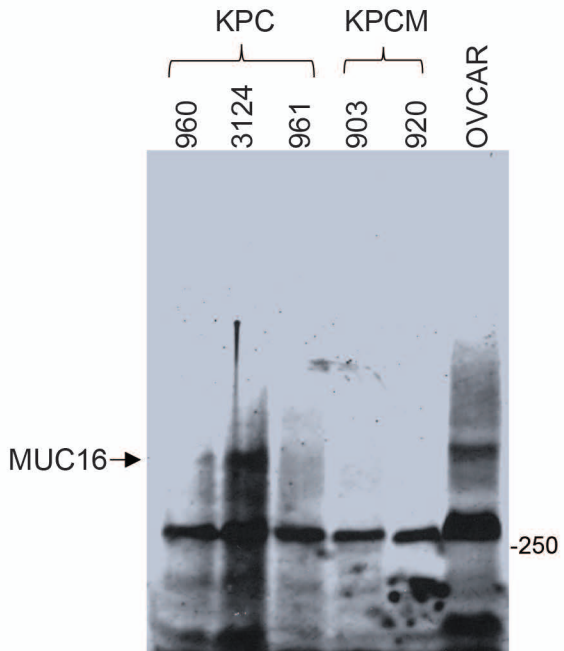
Supplementary Figure 3: **A.** ch5E6 decreased the migration of MUC16 C-ter transfected MiaPaca-2-2 cells as seen by differences in wound area healed in 12 hours than MiaPaca-2-2 vector control cells. **B.** Impact of ch5E6 on the colony formation ability of SW1990 and SW1573 cells by crystal violet staining. Error bars indicate SEM. *, P < 0.05; **, P < 0.005

a**b****c**

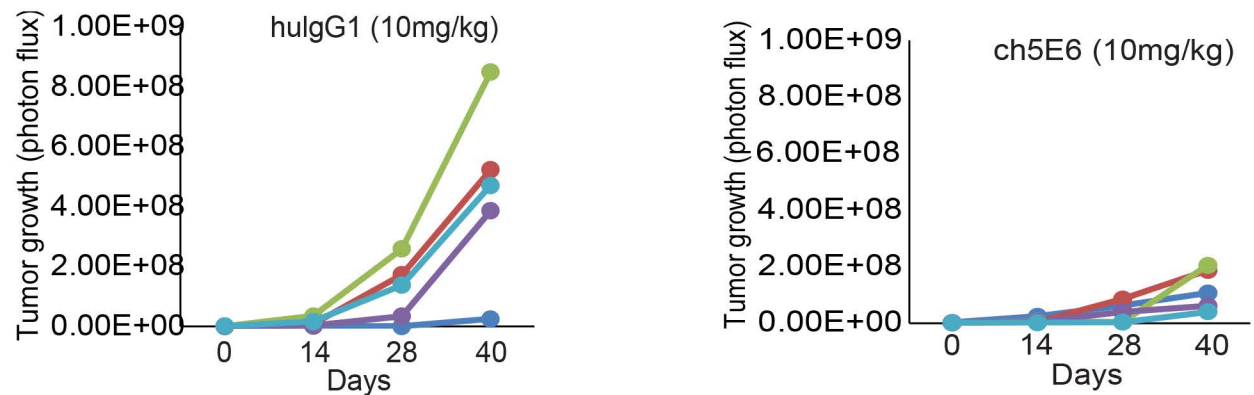
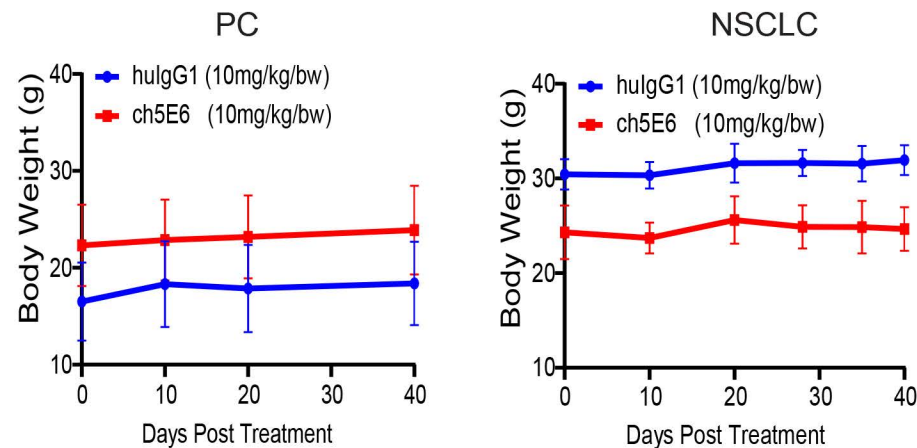
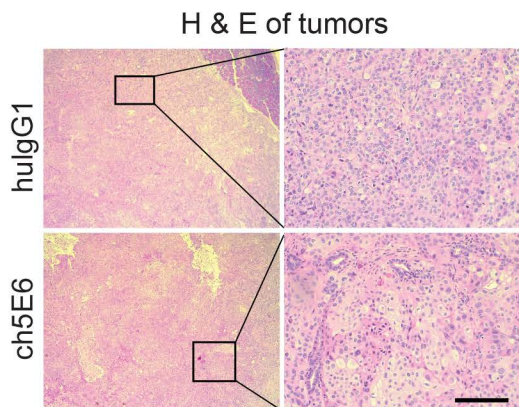
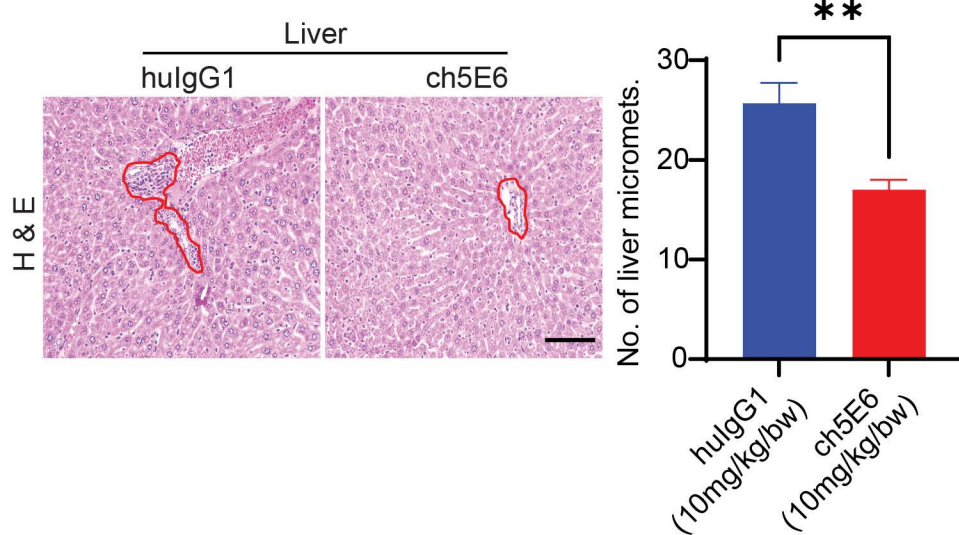
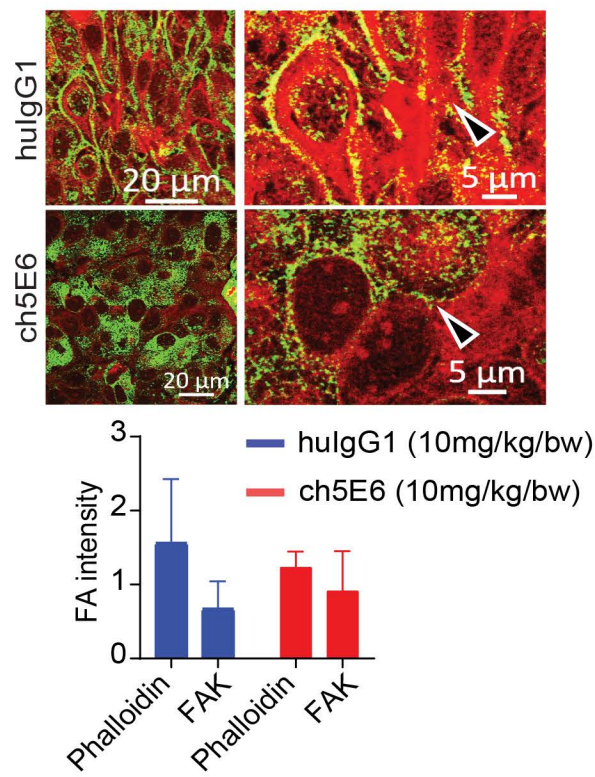
SW1990 (MUC16 knockdown)



Supplementary Figure 4: **A.** Decrease in the fluorescence intensity of N-cadherin by ch5E6 compared to isotype control mAb hulgG1. **B.** The bar graph showing the changes in the expression of various kinases upon treatment with ch5E6 **C.** Immunoblotting analysis of Dox inducible MUC16 knockdown (KD) SW1990 cells showing a decrease in phosphorylated levels of pFAK (Y397), p70S6K, pJNK, and N-cadherin compared to parental cells. Error bars indicate SEM. *, P < 0.05; **, P < 0.005

a**b**

Supplementary Figure 5: **A.** Immunohistochemical staining of ch5E6 in tumor sections from KPC and KPCM (KPCMUC16 knockout) mice indicating a specific reactivity of ch5E6 to mouse MUC16. **B.** Western blot analysis of pancreatic cell lines derived from KPC (960, 3124, and 961) and KPCM (903,920) mice showing mouse MUC16 recognition by ch5E6.

a**b****c****d****e**

Supplementary Figure 6: **A.** The line graphs show the change in flux units for each mouse in the treatment group. **C.** The line graph of body weight measured over various time points showing no changes in the treatment group suggesting a safe profile of the therapy. **D.** H&E images showing low proliferative index in ch5E6 treated tumor than isotype control mAb hulgG1 treated one. **E.** H&E images of liver sections showing a significant decrease in the liver mets in ch5E6 treatment group. **F.** Immunofluorescence analysis of FAK100 stained tumors showing a decrease in focal adhesion intensity in ch5E6 treated tumors as measured by phalloidin and vinculin intensity. Error bars indicate SEM. *, P < 0.05; **, P < 0.005

Supplementary Figure 7 : Full-sized scan of immunoblots in Figure 1 (Fig 1D and Fig 1F)

Figure 1D

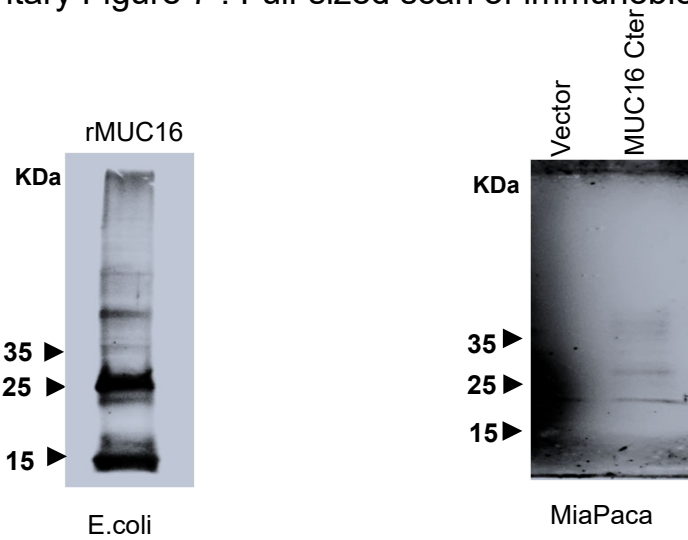
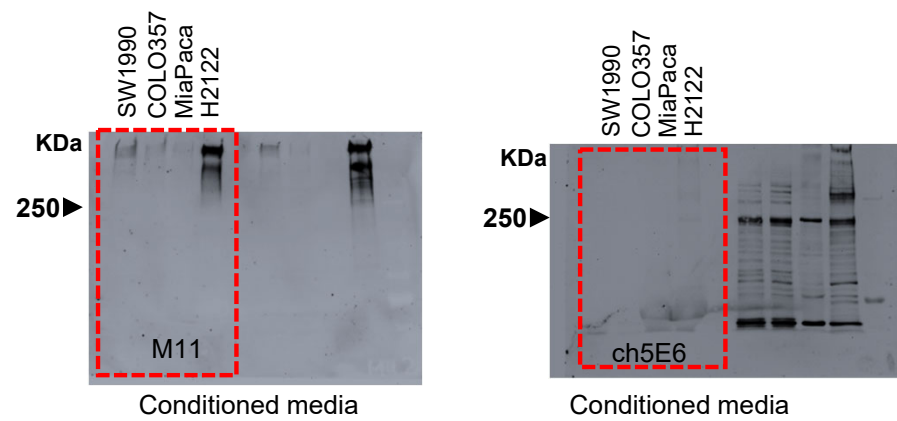
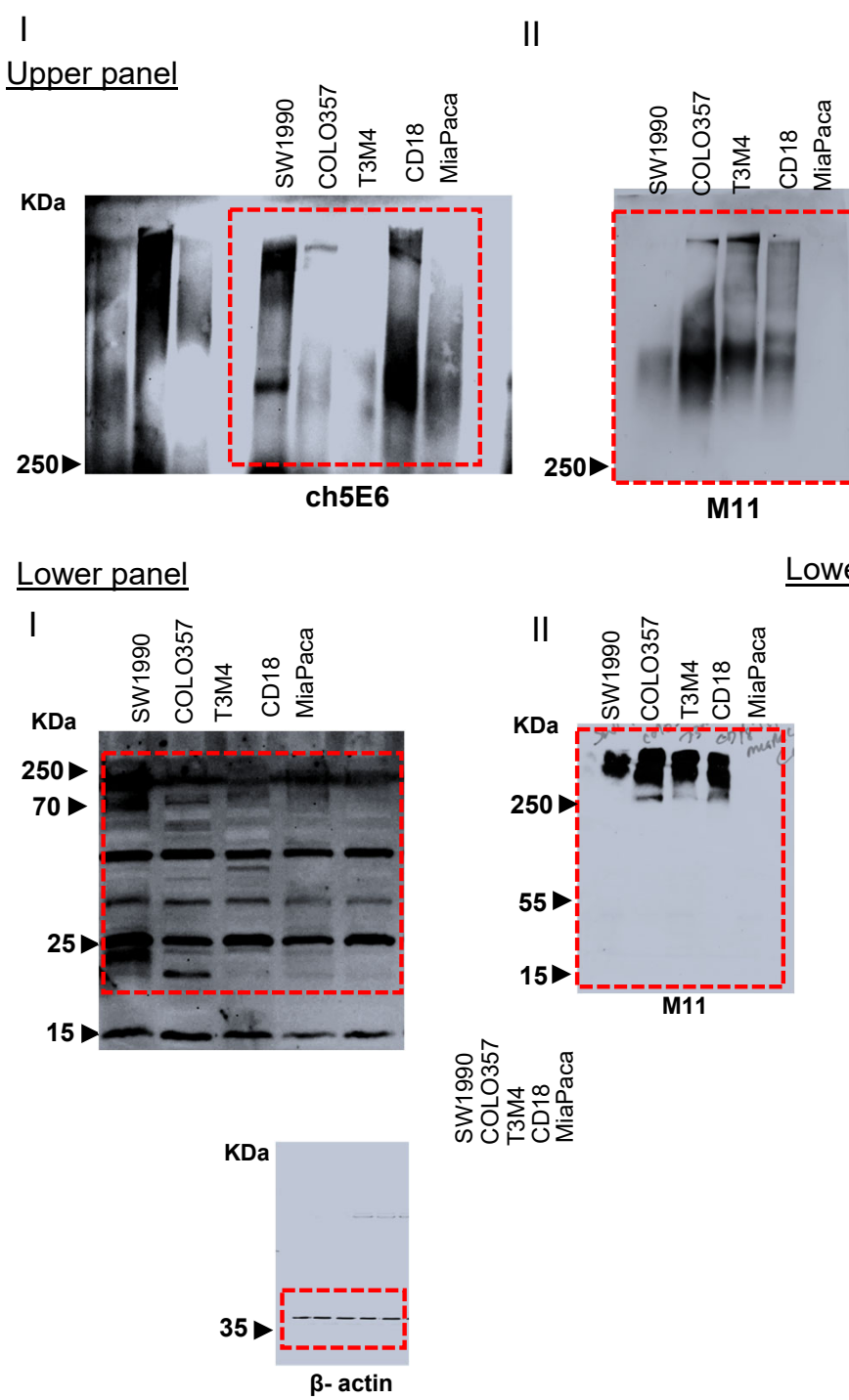


Figure 1F

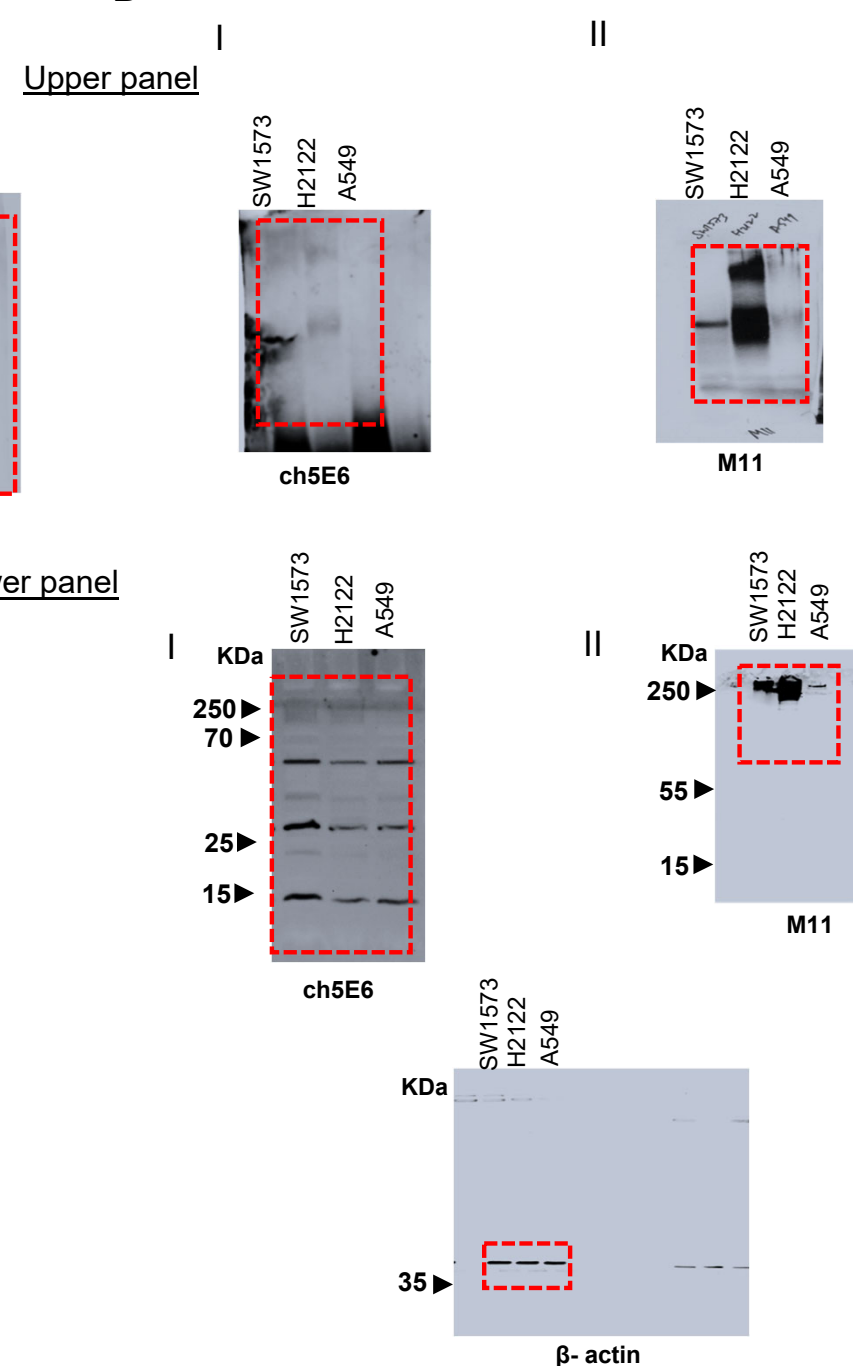


Supplementary Figure 8: Full-sized scan of immunoblots in Figure 2 (Fig 2A and 2B)

A



B



Supplementary Figure 9: Full-sized scan of immunoblots in Figure 3A

Figure 3A (SW1990 Panel)

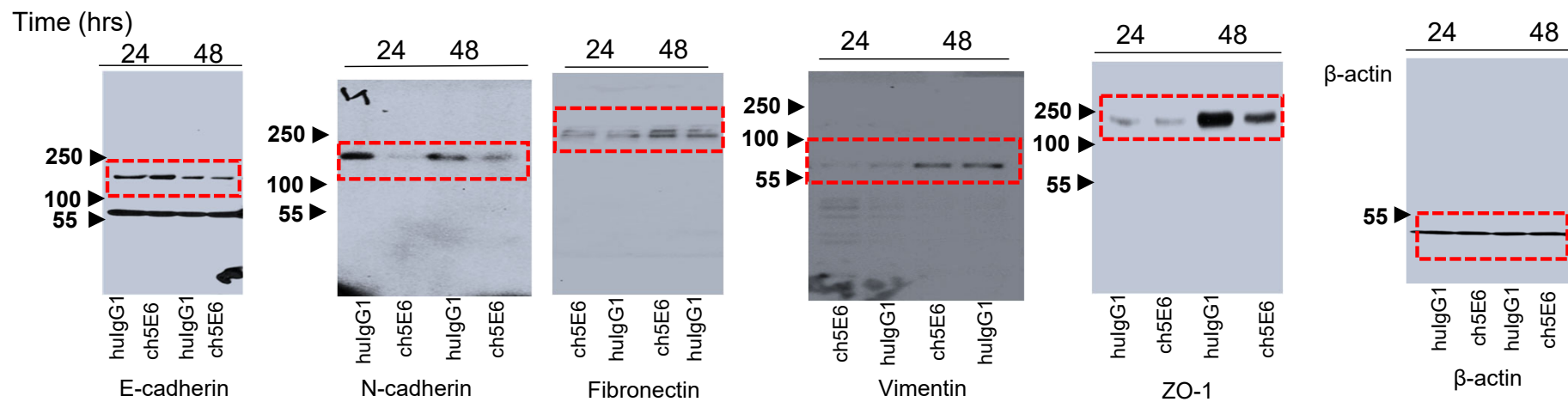
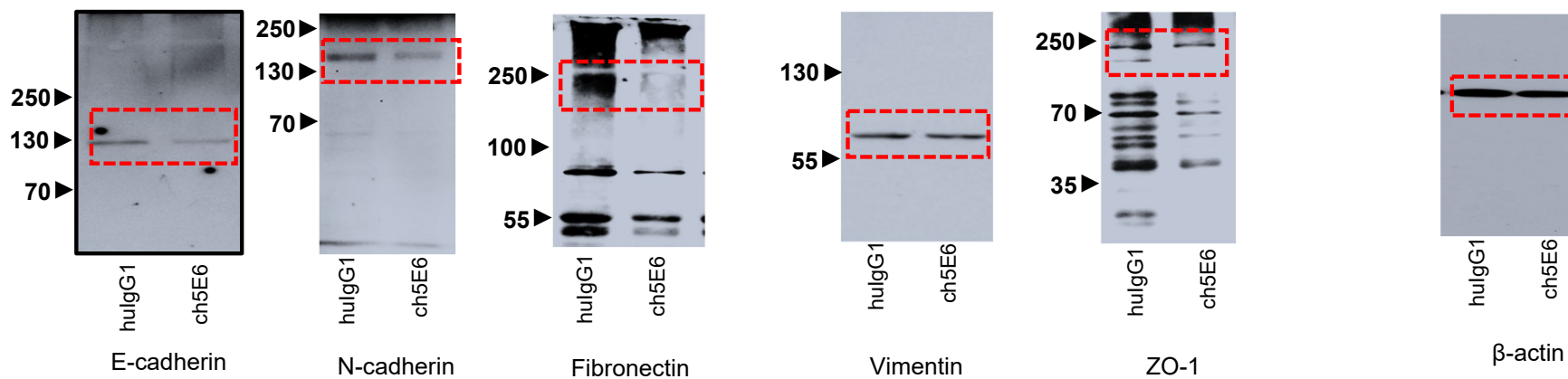
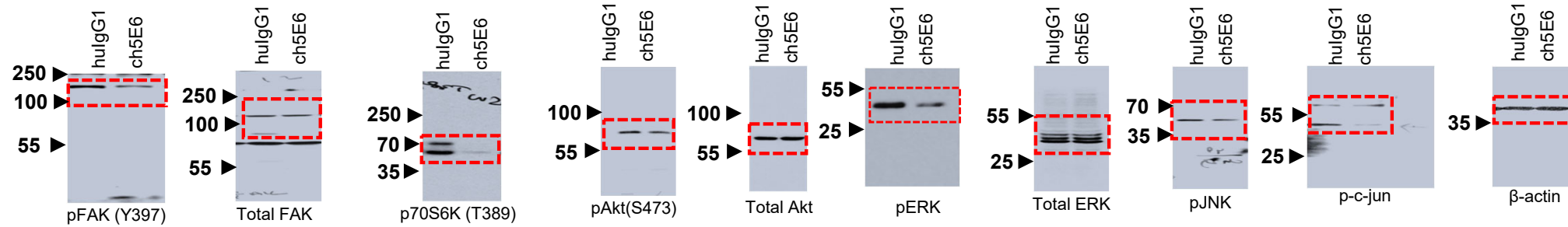


Figure 3A (SW1573 Panel)

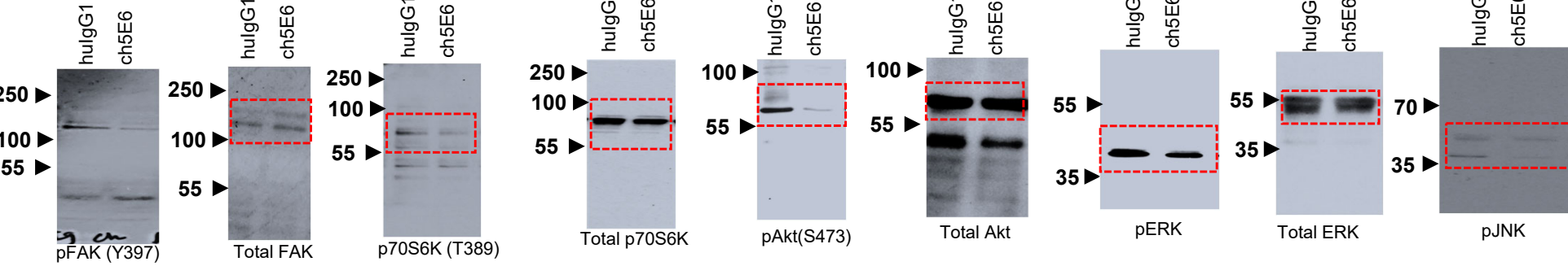


Supplementary Figure 10: Full-sized scan of immunoblots in Figure 3D

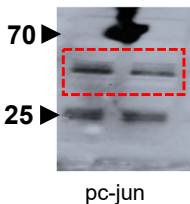
SW1990



SW1573



hulgG1
ch5E6



Supplementary Figure 11: Full-sized scan of immunoblots in Figure 3E, 3F and 3G

Figure 3E

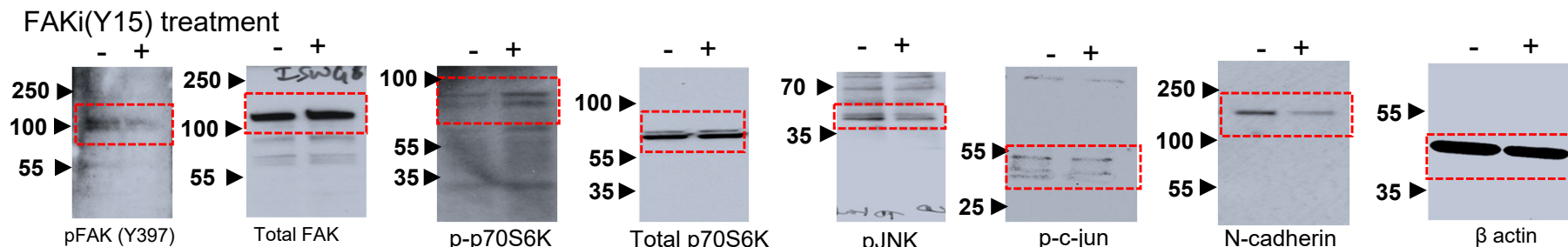


Figure 3F

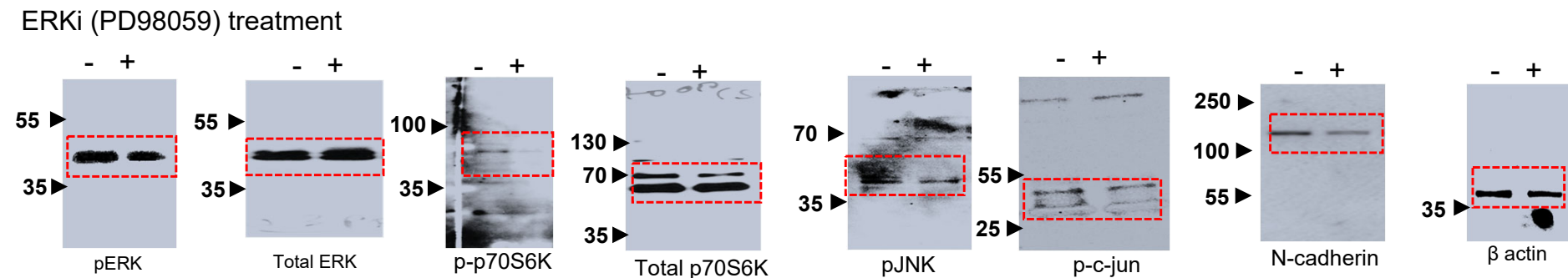
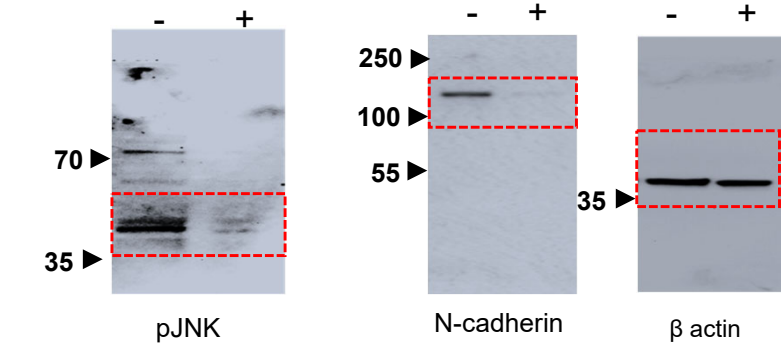


Figure 3G

JNKi (SP60015) treatment



Supplementary Figure 12: Full-sized scan of immunoblots in Figure 6C and D

Figure 6C

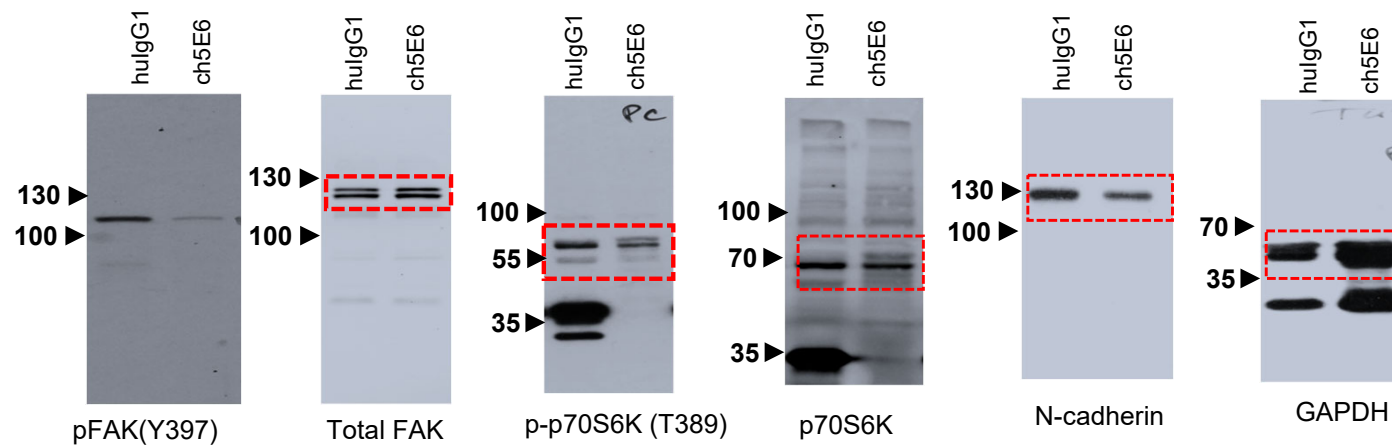
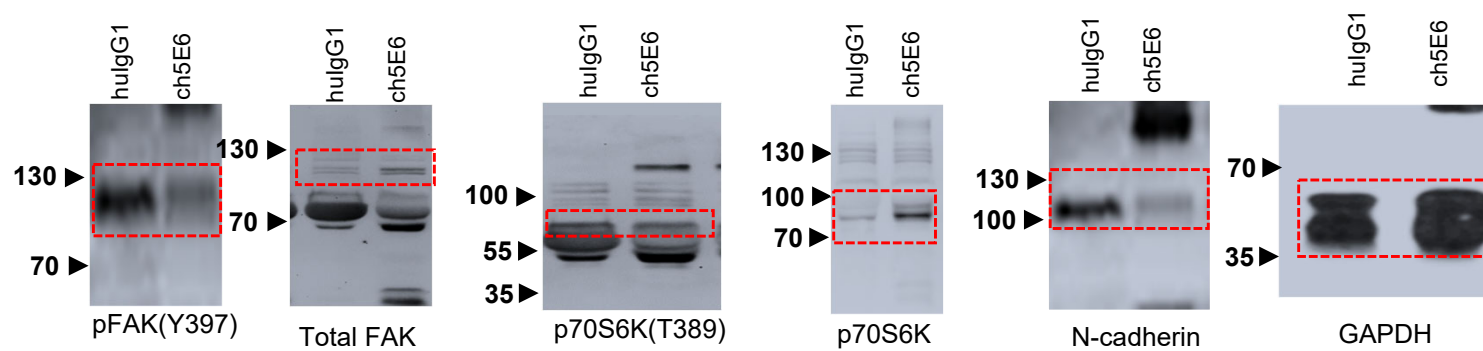
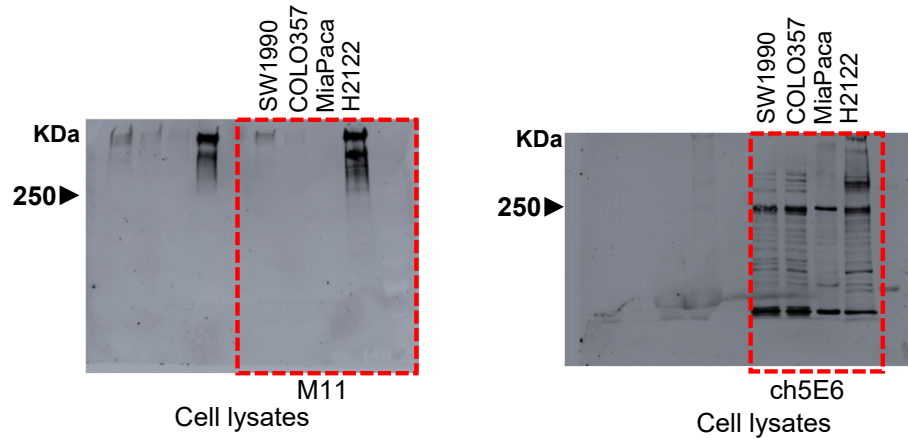


Figure 6D

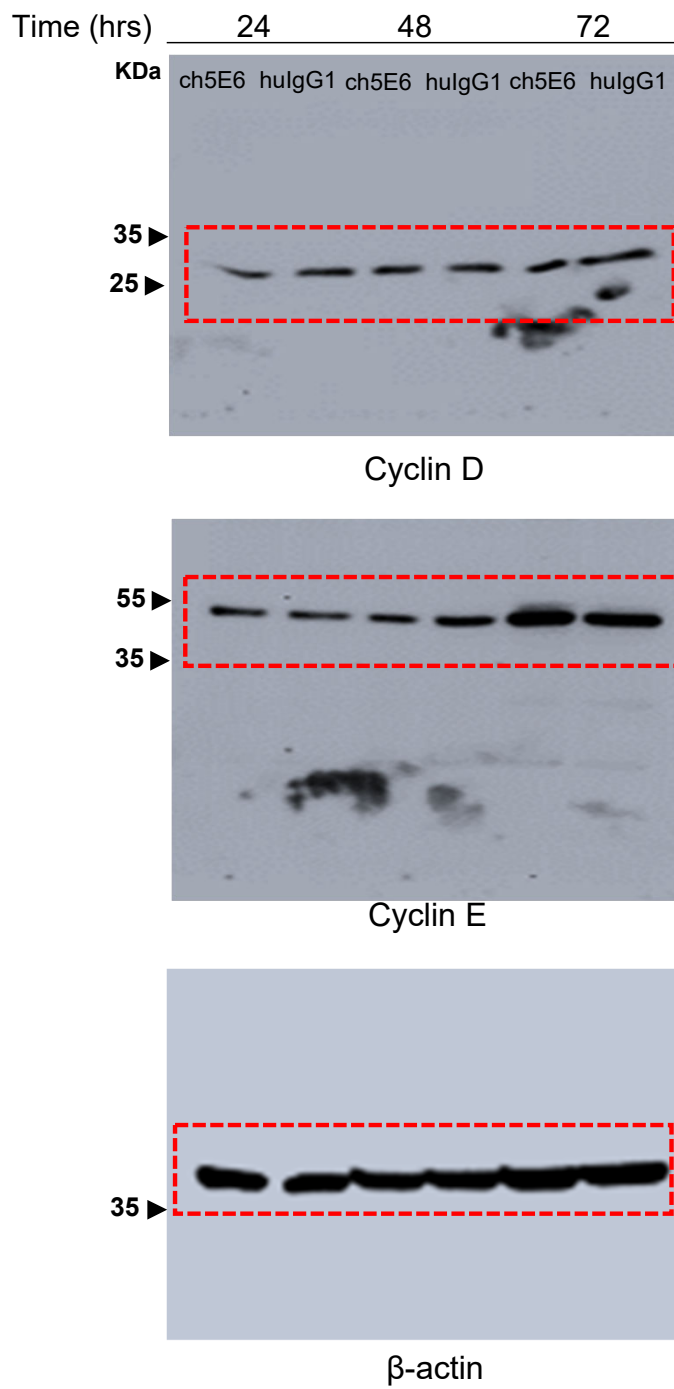


Supplementary Figure 13: Full-sized scan of immunoblots in supplementary figure 1D

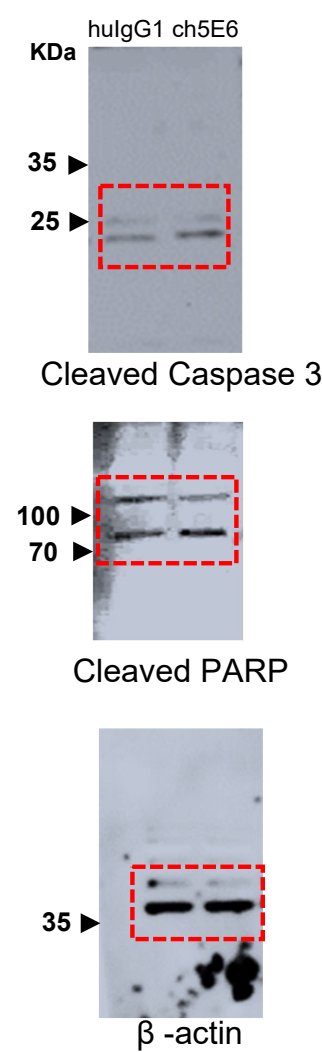


Supplementary Figure 14: Full-sized scan of immunoblots in supplementary figure 2 (S2B, S2E and S2F)

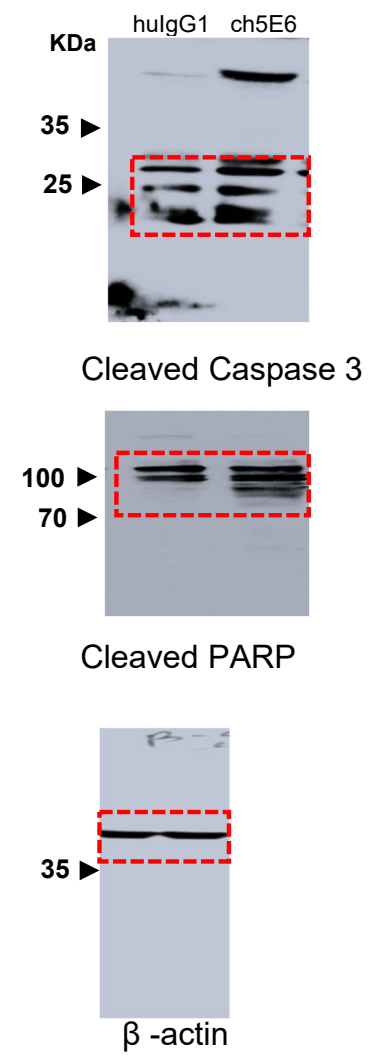
Supplementary Fig 2B



Supplementary Fig 2E



Supplementary Fig 2F



Supplementary Figure 15: Full-sized scan of immunoblots in supplementary Figure 4C

